Published in final edited form as:
J Cogn Neurosci. 2008 June ; 20(6): 1021–1029. doi:10.1162/jocn.2008.20071.

Neural Correlates of Post-error Slowing during a Stop Signal Task: A Functional Magnetic Resonance Imaging Study

Chiang-shan Ray Li, **Cong Huang**, **Peisi Yan**, **Prashni Paliwal**, **Robert Todd Constable**, and **Rajita Sinha**
Yale University

Abstract

The ability to detect errors and adjust behavior accordingly is essential for maneuvering in an uncertain environment. Errors are particularly prone to occur when multiple, conflicting responses are registered in a situation that requires flexible behavioral outputs; for instance, when a go signal requires a response and a stop signal requires inhibition of the response during a stop signal task (SST). Previous studies employing the SST have provided ample evidence indicating the importance of the medial cortical brain regions in conflict/error processing. Other studies have also related these regional activations to postconflict/error behavioral adjustment. However, very few studies have directly explored the neural correlates of post-conflict/error behavioral adjustment. Here we employed an SST to elicit errors in approximately half of the stop trials despite constant behavioral adjustment of the observers. Using functional magnetic resonance imaging, we showed that pre-frontal loci including the ventrolateral prefrontal cortex are involved in post-error slowing in reaction time. These results delineate the neural circuitry specifically involved in error-associated behavioral modifications.

INTRODUCTION

Error detection and behavioral adjustment on the basis of detected errors are an integral component of cortical brain functions. Using various imaging techniques, researchers have tried to understand the neural processes underlying these cognitive events. Many previous studies have localized conflict processing and error detection to the medial frontal cortices (Ridderinkhof, Ullsperger, Crone, & Nieuwenhuis, 2004; Ullsperger & von Cramon, 2004; Ito, Stuphorn, Brown, & Schall, 2003; Van Veen & Carter, 2002; Botvinick, Nystrom, Fissell, Carter, & Cohen, 1999; Carter et al., 1998). Some studies have further elucidated the neural processes linking performance monitoring to behavioral adjustments (Egner & Hirsch, 2004; Ridderinkhof et al., 2004; Durston, Thomas, Worden, Yang, & Casey, 2002; Garavan, Ross, Murphy, Roche, & Stein, 2002). For instance, a functional magnetic resonance imaging (fMRI) study showed that the anterior cingulate cortex (ACC) activates during high conflict situations in a color–word Stroop task and ACC activity is correlated with activation of the dorsolateral prefrontal cortex and with behavioral adjustments during subsequent, postconflict trials (Kerns et al., 2004). These findings support the hypothesis that the engagement of this function leads to the recruitment of cognitive control by the prefrontal cortices (MacDonald, Cohen, Stenger, & Carter, 2000).

However, no studies to our knowledge have directly examined the neural correlates of post-error behavioral adjustment. In the aforementioned study, Kerns et al. (2004) observed greater

Reprint requests should be sent to Chiang-shan Ray Li, Connecticut Mental Health Center, S103, Department of Psychiatry, Yale University School of Medicine, 34 Park Street, New Haven, CT 06519, or via e-mail: chiang-shan.li@yale.edu..

activation of the dorsolateral prefrontal cortex during postconflict but not post-error change in reaction time (RT). Other studies that attempted to examine the neural correlates of post-error behavioral adjustment have not distinguished between adjustment and detection mechanisms (Fiehler, Ullsperger, & von Cramon, 2004; Garavan et al., 2002). For instance, in an fMRI study using a speeded flankers task, participants were either instructed or not instructed to correct their errors (Fiehler et al., 2004). Compared to those who were not instructed to correct errors, those who were instructed to correct errors showed greater activation in the rostral cingulate and pre-supplementary motor areas. However, because error detection necessarily precedes its correction, these results did not distinguish between the two processes. Indeed, these investigators observed activation of similar brain regions during error detection and error correction (Fiehler et al., 2004).

The current study thus attempted to identify the neural substrates of error-related behavioral adjustment. To this aim we employed a stop signal task (SST) widely used to study response inhibition and performance monitoring (Li, Huang, Constable, & Sinha, 2006; Li, Milivojevic, Kemp, Hong, & Sinha, 2006; Aron & Poldrack, 2005; Liotti, Pliszka, Perez, Kothmann, & Woldorff, 2005; Schachar et al., 2004; Logan & Cowan, 1984). The SST requires that observers respond quickly to a frequent signal and withhold their response when a less frequent signal appears. We employed a staircase procedure to ensure that the observers continued to make errors throughout the experiment, despite the ongoing behavioral adjustments following errors. The resultant trial-to-trial variation in the extent of post-error behavioral adjustment enabled us to isolate its neural underpinnings.

METHODS

Subjects and Behavioral Task

Forty healthy adults (20 men, 22−42 years of age, all right-handed, and using their right hand to respond) were paid to participate in the study. All subjects signed a written consent, in accordance to a protocol approved by the Yale Human Investigation Committee.

We employed a simple RT task in this stop signal paradigm (Li, Huang, et al., 2006; Li, Milivojevic, et al., 2006; Figure 1A). There were two trial types: “go” and “stop,” randomly intermixed. A small dot appeared on the screen to engage attention and eye fixation at the beginning of a go trial. After a randomized time interval anywhere between 1 and 5 sec, the dot turned into a circle, which subtended approximately 2° of visual angle. The circle served as an imperative stimulus and the subjects were instructed to quickly press a button at the “go” signal but not before. The circle vanished at button press or after 1 sec had elapsed, whichever came first, and the trial terminated. A premature button press prior to the appearance of the circle also terminated the trial. Three quarters of all trials were go trials. The remaining one quarter were stop trials. In a stop trial, an additional “X,” the “stop” signal, appeared after and replaced the go signal. The subjects were told to withhold button press upon seeing the stop signal. Likewise, a trial terminated at button press or when 1 sec had elapsed since the appearance of the stop signal. Clearly, it would be easier for the subject to withhold the response if the stop signal appeared immediately or early after the go signal, and the reverse applied if the time interval between the stop and the go signals (or the stop signal delay, SSD) was extended. The SSD started at 200 msec and varied from one stop trial to the next according to a staircase procedure: If the subject succeeded in withholding the response, the SSD increased by 64 msec; conversely, if they failed, SSD decreased by 64 msec (Levitt, 1970). There was an intertrial interval of 2 sec. Subjects were instructed to respond to the go signal quickly while keeping in mind that a stop signal could come up in a small number of trials. Prior to the fMRI study, each subject had a practice session outside the scanner. The duration of practice session varied, with most subjects understanding the task very well within approximately 5 min of practice (i.e., 50 trials during the SST). During the practice session, almost all subjects learned

to slow down after they encountered stop errors. At that point, they were explicitly instructed that it made sense for them to slow down because they knew that a stop signal could come up in some trials. However, it was also emphasized to them that they could not slow down to such an extent that they would miss the time window to respond to the go signal. They were instructed that it would count as an error if they waited until the go signal (the circle) disappeared from the screen and that they should respond to the circle well before that happened. A few subjects pointed out the tradeoff between "wait" and "respond quickly." They were ensured that there was, indeed, such a tradeoff and their best strategy really was just to pay attention: "Be relatively fast in responding to the circle, while keeping in mind that a stop signal could come up in come trials."

In the scanner, each subject completed four 10-min runs of the task with the SSD updated manually across runs. Depending on the actual stimulus timing (trial varied in fore-period duration) and speed of response, the total number of trials varied slightly across subjects in an experiment (averaging approximately 315 go and 105 stop trials). With the staircase procedure, we anticipated that the subjects succeeded in withholding their response in approximately half of the stop trials.

Imaging Protocol

Conventional T1-weighted spin echo sagittal anatomical images were acquired for slice localization using a 3-T scanner (Siemens Trio). Anatomical images of the functional slice locations were next obtained with spin-echo imaging in the axial plane parallel to the AC–PC line with TR = 300 msec, TE = 2.5 msec, bandwidth = 300 Hz/pixel, flip angle = 60°, field of view = 220 × 220 mm, matrix = 256 × 256, 32 slices with slice thickness = 4 mm, and no gap. Functional, blood oxygenation level-dependent (BOLD) signals were then acquired with a single-shot, gradient-echo, echo-planar imaging (EPI) sequence. Thirty-two axial slices parallel to the AC–PC line covering the whole brain were acquired with TR = 2000 msec, TE = 25 msec, bandwidth = 2004 Hz/pixel, flip angle = 85°, field of view = 220 × 220 mm, matrix = 64 × 64, 32 slices with slice thickness = 4 mm, and no gap. Three hundred images were acquired in each run for a total of 4 runs.

Data Analysis and Statistics

Data were analyzed with Statistical Parametric Mapping version 2 (SPM2, Welcome Department of Imaging Neuroscience, University College London, UK). Images from the first five TRs at the beginning of each trial were discarded to enable the signal to achieve steady-state equilibrium between RF pulsing and relaxation. Images of each individual subject were first corrected for slice timing and realigned (motion-corrected). A mean functional image volume was constructed for each subject for each run from the realigned image volumes. These mean images were normalized to an MNI (Montreal Neurological Institute) EPI template with affine registration followed by nonlinear transformation (Ashburner & Friston, 1999; Friston, Ashburner, et al., 1995). The normalization parameters determined for the mean functional volume were then applied to the corresponding functional image volumes for each subject. Finally, images were smoothed with a Gaussian kernel of 10 mm at full width at half maximum. The data were high-pass filtered (1/128 Hz cutoff) to remove low-frequency signal drifts.

Four main types of trial outcome were first distinguished: go success (G), go error (F), stop success (SS), and stop error (SE) trial (Figure 1B). An SS or SE trial involves incongruent goals between the prepotency to respond and the motor intention to withhold the response, and thus, is "high-conflict," compared to a G trial. G trials were divided into those that followed a G (pG), F (pF), SS (pSS), and SE (pSE) trial, and pSS and pSE trials were further divided into those that increased in RT (pSSi and pSEi, respectively) and those that did not increase in RT (pSSni and pSEni), to allow the isolation of neural processes involved in postconflict/error

behavioral adjustment. To determine whether a pSS/pSE trial increased or did not increase in RT, it was compared to the pG trials that preceded it in time during each session. The pG trials that followed the pSS or pSE trial were not included for comparison because the neural/cognitive processes associated with these pG trials occurred subsequent to, and thus, could not have a causal effect on the pSS or pSE trial. A single statistical analytical design was constructed for each individual subject, using the general linear model (GLM) with the onsets of go signal in each of these trial types convolved with a canonical hemodynamic response function (HRF) and with the temporal derivative of the canonical HRF and entered as regressors in the model (Friston, Holmes, et al., 1995). Realignment parameters in all six dimensions were also entered in the model. Serial autocorrelation of the time series caused by aliased cardiovascular and respiratory effects violated the GLM assumption of the independence of the error term and was corrected by a first-degree autoregressive or AR(1) model (Della-Maggiore, Chau, Peres-Neto, & McIntosh, 2002; Friston et al., 2000). The GLM estimated the component of variance that could be explained by each of the regressors.

In the first-level analysis, we constructed for each individual subject two contrasts: pSSi versus pSSni, and pSEi versus pSEni, to identify activations associated with post-conflict and post-error adjustment in RT, respectively. The contrast images were then used for random effect analysis (Penny & Holmes, 2004). Brain regions were identified using an atlas (Mai, Paxinos, & Asheuer, 2003). In region-of-interest (ROI) analysis, we used MarsBaR (Brett, Anton, Valabregue, & Poline, 2002; http://marsbar.sourceforge.net/) to derive for each individual subject the effect size of activity change for the ROIs. The functional ROIs were defined based on activated clusters from whole-brain analysis. All voxel activations are presented in MNI coordinates.

RESULTS

General Behavioral Performance

General behavioral results are listed in Table 1a. The mean and median go trial RT were 547 ± 115 msec (mean ± *SD*) and 538 ± 122 msec, respectively, consistent with the right-skewed distribution of RT in an RT task. Furthermore, we performed for each individual observer a linear regression between the RT and stop signal delay (SSD) across all stop error (SE) trials. The results showed that the RT and SSD were highly correlated (r ranged from .58 to .94, all ps < .0001, Pearson regression), providing more evidence for the success of the tracking procedure.

We further examined whether post-stop go trial performance is related to the conditions of the preceding stop trial. Table 1b shows the SSD and RT of SE trials, separately for pSEi and pSEni trials (i.e., SE trials grouped according to whether its subsequent trial is a pSEi or pSEni; SSD: $p = .414$; RT: $p = .179$, paired t test), and the SSD of SS trials, separately for pSSi and pSSni trials ($p < .863$, paired t test). Moreover, linear regressions showed that across all subjects for pSEi trials, RT increase was not correlated with the SSD ($p = .077$) or RT ($p = .296$) of the SE trials; for pSEni trials, RT decrease was not correlated with the SSD ($p = .078$) or RT ($p = .238$) of the SE trials; for pSSi and pSSni trials, RT increase and decrease, respectively, did not correlate with the SSD of the preceding SS trial ($p = .174$ and .397). Overall, these results suggest that the RT change in post-stop go trials are not influenced by the parametric conditions of their preceding stop trials.

Neural Substrates of Post-error Behavioral Adjustment

We examined which specific brain regions are involved during post-error adjustment in RT. Our observers exhibited a robust post-stop error slowing effect: RTs were significantly slower on pSE trials compared to pG trials (570 ± 127 vs. 528 ± 121 msec, mean ± *SD*; $p < .001$, paired

t test; Figure 1C), suggesting that they implemented appropriate error monitoring and adjusted behaviors accordingly (Rabbit, 1966). Importantly, although observers were generally slower responding after an error, individual participants demonstrated significant trial-to-trial variation in pSE slowing. We took advantage of this within-subject variability and compared pSE trials with (69 ± 13%; mean ± *SD* across all observers; RT increase = 124 ± 39 msec; mean ± *SD*, across all observers) and without (31 ± 13%; RT decrease = 72 ± 40 msec) RT slowing. We observed that the right ventrolateral prefrontal cortex (VLPFC: $x = 44$ mm, $y = 24$ mm, $z = -4$ mm, BA 47; $Z = 4.87$, 1792 mm^3) was significantly more activated during pSE trials with RT slowing than during pSE trials without RT slowing (i.e., pSEi > pSEni, $p < .05$, corrected for family-wise errors during multiple comparisons; Figure 2A). However, the VLPFC activation did not correlate with the extent of pSE slowing across subjects ($r = .094$, $p = .564$, Pearson regression for all 40 subjects; $r = 0.005$, $p = .976$, Pearson regression for those who showed positive pSE slowing; $n = 36$; Figure 2B). At a lower statistical threshold ($p < .05$, corrected for false discovery rate or FDR; Genovese, Lazar, & Nichols, 2002), the left VLPFC and other right prefrontal structures also showed greater activation during pSEi, compared to pSEni trials (Table 2). Conversely, no brain regions showed greater activation during pSEni than during pSEi trials ($p < .01$, uncorrected).

Interestingly, our observers demonstrated similar RT slowing during pSS trials, compared to pSE slowing (562 ± 126 vs. 570 ± 127 msec, $p > .1$, paired *t* test; Figure 1C). However, pSS trials with (64 ± 15%, RT increase = 112 ± 35 msec, mean ± *SD*, across all observers) and without (36 ± 15%, RT decrease = 71 ± 30 msec, mean ± *SD*, across all observers) RT slowing did not differ in regional brain activation even at a lower significance threshold (no voxels survived $p < .01$, uncorrected, for either direction).

This raised the question of whether pSE slowing is due to distinctly different neural circuitry from pSS slowing. That is, is there an error-specific mechanism during behavioral adjustment? We compared these two conditions directly (i.e., [pSEi–pSEni] vs. [pSSi–pSSni]) and, in addition to the right VLFPC ($x = 40$ mm, $y = 24$ mm, $z = -8$ mm, $Z = 4.04$, 5248 mm^3), found greater activation in the right middle frontal ($x = 56$ mm, $y = 20$ mm, $z = 36$ mm; BA 9; $Z = 3.65$, 3328 mm^3) and fronto-polar ($x = 44$ mm, $y = 52$ mm, $z = 12$ mm; BA 10; $Z = 3.63$, 1024 mm^3) gyri during pSE slowing compared to pSS slowing ($p < .001$, uncorrected, and 10 voxels in extent of activation; Figure 3). Activation of the three brain regions were highly correlated across subjects during post-error slowing ($.58 < r < .63$; all *p*s < .001, pairwise Pearson regressions). The left VLPFC ($x = -40$ mm, $y = 12$ mm, $z = -12$ mm; $Z = 2.82$, 1216 mm^3) also showed greater activation during pSE slowing, compared to pSS slowing, at $p < .01$, uncorrected.

To further examine the specificity of these findings, we distinguished in a second GLM post-go or pG trials with RT slowing (pGi trials) and those without RT slowing (pGni trials). This statistical model of the time series allowed us to examine pSE and pSS slowing, as compared to pG slowing. Thus, by contrasting “pSEi–pSEni” and “pGi–pGni,” we obtained greater activation in the right VLPFC ($x = 48$ mm, $y = 20$ mm, $z = -8$ mm; voxel $Z = 5.13$, 832 mm^3) and middle frontal cortex ($x = 52$ mm, $y = 28$ mm, $z = 32$ mm; $Z = 4.16$, 320 mm^3), at a $p < .05$, corrected for FDR, and 5 voxels in the extent of activation. No regions showed greater activation during pGi–pGni than pSEi–pSEni, even at an uncorrected $p < .01$. These results are thus almost identical to those obtained with pSE slowing versus pSS slowing. In contrast, no brain regions demonstrated greater activation during pSS slowing as compared to pG slowing or vice versa at the same statistical thresholds.

DISCUSSION

We have shown greater activation in the right VLPFC during post-stop error (pSE) slowing in RT. Because the two groups of pSE trials are identical in all aspects other than RT, the VLPFC activation is associated specifically with cognitive–motor processes during RT slowing. The VLPFC is connected with other prefrontal and pre-motor circuitry and has been implicated in many previous studies in mediating attention and action reversals (Hampshire & Owen, 2006; Weissman, Roberts, Visscher, & Woldorff, 2006; Shafritz, Kartheiser, & Belger, 2005; Swainson et al., 2003; Cools, Clark, Owen, & Robbins, 2002). For instance, during a task in which participants learned arbitrary stimulus–response associations, this brain region activated specifically when they stopped responding to the previously relevant stimulus and shifted responding to the newly relevant stimulus (Cools et al., 2002). The VLPFC activation during pSE slowing thus appears to reflect the decision to reverse the prepotent response tendency and to slow down after observers encounter an error. This control-level mechanism also appears to be supported by a lack of correlation between the VLPFC activation and the extent of pSE slowing (a positive correlation would suggest a “peripheral,” effector-level mechanism that mediates trial-to-trial variation in activity of the motor apparatus).

The left VLPFC also showed greater activation during pSE slowing, although to a lesser extent compared to the right VLPFC. The bilateral VLPFC was involved in switching attention between stimulus dimensions in an earlier study using a face/building target identification task (Hampshire & Owen, 2006). Another study showed bilateral VLPFC activation during a memory task, in which observers were instructed to remember stimuli on pictures of abstract art, compared to when they were not explicitly so instructed (Dove, Brett, Cusack, & Owen, 2006). Bilateral mid-VLPFC activation was also observed during target identification regardless of context, in contrast to the DLPFC which activated during contextual evaluation and integration of information (Rahm et al., 2006). Exclusively, right hemispheric VLPFC activation was found during task switching in a paradigm in which subjects made compatible left/right keypress responses to left/right arrow stimuli under two trial conditions of responding —at stimulus onset and stimulus offset—between which they switched every two trials (Swainson et al., 2003). Right but not left VLPFC showed greater activation in the aforementioned study of Cools et al. (2002), during which subjects shifted response to a newly relevant stimulus. In contrast, in a different behavioral task in which subjects must attend to rule and object switch, the left VLFPC showed greater activation during such switching (Cools, Clark, & Robbins, 2004). Note that in this latter study subjects responded to the stimuli (rule and object) that could constantly change and did not appear obliged to set up a prepotent response tendency, as in probabilistic reversal-learning task (Cools et al., 2002). Other studies have also isolated the left but not the right VLPFC during resolution of proactive interference or conceptual conflict in a variety of behavioral tasks and during rule retrieval when a response contingency continued to be maintained (Badre & Wagner, 2006; Badre, Poldrack, Paré-Blagoev, Insler, & Wagner, 2005; Bunge, Kahn, Wallis, Miller, & Wagner, 2003). Taken together, these previous studies broadly suggest that the left VLPFC is involved in attentional monitoring during stimulus/memory/rule processing, whereas the right VLPFC is engaged more clearly during a process in which a change from a prepotent rule/response tendency is required. Thus, during pSE slowing, both prefrontal structures are engaged in this attention-demanding process involving reversal of the prepotent quick response to the go signal.

The right middle frontal and fronto-polar cortices also activated during pSE slowing. Allowing certain anatomical flexibility, these two brain regions have been implicated in many cognitive processes, including working memory, attention, and executive processes such as stimulus manipulation and subgoaling (see Burgess, Gilbert, & Dumontheil, 2007; Wager & Smith, 2003; Wagner, 1999 for reviews). Thus, simple as it seems, pSE slowing may invoke other

cognitive processes that do not show behaviorally and that require investigation in further studies.

On the other hand, no specific brain regions activated during post-stop success (pSS) slowing in response. This finding suggests that postconflict adjustment in RT can involve more than one single process. One can perhaps speculate that instead of being carried out by an active decision, pSS slowing could reflect motor hesitancy, as a result of a lack of decision or "not knowing what to do" while observers continue to process the alerting effect of the stop trial. That is, observers slow down following a stop success not because of implementation of cognitive control but because of "conflicting" information processing which, as a result, delays the response. It is of interest to contrast this scenario with the color–word Stroop task, in which Kerns et al. (2004) observed prefrontal activation primarily during postconflict behavioral adjustment. Behavioral adjustment in this Stroop study reflected primarily faster RT in incongruent trial following an incongruent trial (i.e., iI trial), compared to an incongruent trial following a congruent trial (i.e., cI trial). It appears that an active control process evoked during incongruency processing expedites the processing of conflicting information and, as a result, shortens the RT during subsequent trials. In our SST, because low-conflict go trials follow the high-conflict stop trials most of the time, any control process engaged during stop successes may not exert any advantageous effect despite the additional cost in processing. Thus, two points are worth noting from this comparison of the current results and those of Kerns et al. First, postconflict change in RT does not necessarily occur as a result of cognitive control. Second, the prefrontal cortex appears to activate only when cognitive control is actively implemented.

In the above discussions, we distinguished stop successes and stop errors as if they each distinctly involve conflict and error processing, respectively. Such an assumption is oversimplified as conflicting motor responses (and thus, conflict processing) are engaged during error trials. In search for an error-specific process, thus, we contrasted pSE slowing and pSS slowing and, at a lower significance threshold (compared to VLPFC activation during pSE slowing), observed activation of additional prefrontal regions. These right hemispheric cortical structures thus appear to mediate error-specific behavioral adjustment. This lateralization of the error-specific control system is consistent with a recent report demonstrating that disruption of the right but not the left prefrontal cortex by transcranial magnetic stimulation increases risk-taking behaviors during a gambling task, suggesting that alterations in right pre-frontal activation can lead to impaired error-contingent control during high-level decision making (Knoch et al., 2006). On the other hand, as we have discussed earlier, it is not clear what processes account for pSS slowing; thus, the dorsolateral prefrontal and fronto-polar cortices identified from the contrast of pSE slowing versus pSS slowing may involve multiple psychological constructs. For instance, although the right fronto-polar cortex is implicated in cognitive control and decision making, this brain region has also been shown to activate to prospective memory, item familiarity in contrast to contextual recollection, and "subgoaling" during a working memory task, to name a few recent findings (den Ouden, Frith, Frith, & Blakemore, 2005; Yarkoni et al., 2005; Badre & Wagner, 2004; Dobbins, Simons, & Schacter, 2004; Burgess, Scott, & Frith, 2003; Braver & Bongiolatti, 2002). The exact role these prefrontal structures play in post-error behavioral adjustment would await clarification of the psychological and neural processes involved in pSS slowing.

Another issue of note is that behavioral adjustment in different "cognitive control" tasks may involve very different outcome measures. In the current as well as many of the aforementioned studies, behavioral adjustment is defined solely in terms of RT change following an error or high-conflict situation. However, many other studies required adjustment by, for instance, attending to a different stimulus–response rule, which entailed behavioral outcomes that could not be as readily captured by RT changes (Crone, Wendelken, Donohue, & Bunge, 2006;

Liston, Matalon, Hare, Davidson, & Casey, 2006; Walton, Devlin, & Rushworth, 2004). Thus, one might expect different prefrontal mechanisms to be engaged during behavioral adjustment with respect to the specificity of task requirement.

In conclusion, using a tracking SST, we have specifically identified the neural correlates of post-error slowing. These results thus elucidate an additional aspect of the role of the prefrontal cortex in post-error behavioral adjustment.

Acknowledgments

This study was supported by the Yale Interdisciplinary Women's Health Research Scholar Program on Women and Drug Abuse (C.-S. R. L.), funded by the NIH Office of Research on Women's Health and the National Institute on Drug Abuse, and NIH grants (R. S., C.-S. R. L.). This project was also funded in part by the State of Connecticut, Department of Mental Health and Addictions Services. We thank Mark Laubach, Daeyeol Lee, James Mazer, Nandakumar Narayanan, Camillo Padoa-Schioppa, and Maolin Qiu for their most helpful discussions and comments on an earlier version of the manuscript.

REFERENCES

Aron AR, Poldrack RA. The cognitive neuroscience of response inhibition: Relevance for genetic research in attention-deficit/hyperactivity disorder. Biological Psychiatry 2005;57:1285–1292. [PubMed: 15950000]

Ashburner J, Friston KJ. Nonlinear spatial normalization using basis functions. Human Brain Mapping 1999;7:254–266. [PubMed: 10408769]

Badre D, Wagner AD. Selection, integration, and conflict monitoring; assessing the nature and generality of prefrontal cognitive control mechanisms. Neuron 2004;41:473–487. [PubMed: 14766185]

Badre D, Wagner AD. Computational and neurobiological mechanisms underlying cognitive flexibility. Proceedings of the National Academy of Sciences, U.S.A 2006;103:7186–7191.

Badre D, Poldrack RA, Paré-Blagoev EJ, Insler RZ, Wagner AD. Dissociable controlled retrieval and generalized selection mechanisms in ventrolateral prefrontal cortex. Neuron 2005;47:907–918. [PubMed: 16157284]

Botvinick M, Nystrom LE, Fissell K, Carter CS, Cohen JD. Conflict monitoring versus selection-for-action in anterior cingulate cortex. Nature 1999;402:179–181. [PubMed: 10647008]

Braver TS, Bongiolatti SR. The role of frontopolar cortex in subgoal processing during working memory. Neuroimage 2002;15:523–536. [PubMed: 11848695]

Brett, M.; Anton, J-L.; Valabregue, R.; Poline, J-P. Region of interest analysis using an SPM toolbox.. Abstract presented at the 8th International Conference on Functional Mapping of the Human Brain; Sendai, Japan. June 2–6; 2002.

Bunge SA, Kahn I, Wallis JD, Miller EK, Wagner AD. Neural circuits subserving the retrieval and maintenance of abstract rules. Journal of Neurophysiology 2003;90:3419–3428. [PubMed: 12867532]

Burgess PW, Gilbert SJ, Dumontheil I. Function and localization within rostral prefrontal cortex (area 10). Philosophical Transactions of the Royal Society of London, Series B, Biological Sciences 2007;362:887–899.

Burgess PW, Scott SK, Frith CD. The role of the rostral frontal cortex (area 10) in prospective memory: A lateral versus medial dissociation. The role of the rostral frontal cortex (area 10) in prospective memory: A lateral versus medial dissociation. Neuropsychologia 2003;41:906–918. [PubMed: 12667527]

Carter CS, Braver T, Barch D, Botvinick M, Noll D, Cohen JD. Anterior cingulate cortex, error detection, and the online monitoring of performance. Science 1998;280:747–749. [PubMed: 9563953]

Cools R, Clark L, Owen AM, Robbins TW. Defining the neural mechanisms of probabilistic reversal learning using event-related functional magnetic resonance imaging. Journal of Neuroscience 2002;22:4563–4567. [PubMed: 12040063]

Cools R, Clark L, Robbins TW. Differential responses in human striatum and prefrontal cortex to changes in object and rule relevance. Journal of Neuroscience 2004;24:1129–1135. [PubMed: 14762131]

Crone EA, Wendelken C, Donohue SE, Bunge SA. Neural evidence for dissociable components of task-switching. Cerebral Cortex 2006;16:475–486. [PubMed: 16000652]

Della-Maggiore V, Chau W, Peres-Neto PR, McIntosh AR. An empirical comparison of SPM preprocessing parameters to the analysis of fMRI data. Neuroimage 2002;17:19–28. [PubMed: 12482065]

den Ouden HE, Frith U, Frith C, Blakemore SJ. Thinking about intentions. Neuroimage 2005;28:787–796. [PubMed: 15964210]

Dobbins IG, Simons JS, Schacter DL. fMRI evidence for separable and lateralized prefrontal memory monitoring processes. Journal of Cognitive Neuroscience 2004;16:908–920. [PubMed: 15298779]

Dove A, Brett M, Cusack R, Owen AM. Dissociable contributions of the mid-ventrolateral frontal cortex and the medial temporal lobe system to human memory. Neuroimage 2006;31:1790–1801. [PubMed: 16624583]

Durston S, Thomas KM, Worden MS, Yang Y, Casey BJ. The effect of preceding context on inhibition: An event-related fMRI study. Neuroimage 2002;16:449–453. [PubMed: 12030830]

Egner T, Hirsch J. The neural correlates and functional integration of cognitive control in a Stroop task. Neuroimage 2004;24:539–547. [PubMed: 15627596]

Fiehler K, Ullsperger M, von Cramon DY. Neural correlates of error detection and error correction: Is there a common neuroanatomical substrate? European Journal of Neuroscience 2004;19:3081–3087. [PubMed: 15182316]

Friston KJ, Ashburner J, Frith CD, Polone J-B, Heather JD, Frackowiak RSJ. Spatial registration and normalization of images. Human Brain Mapping 1995;2:165–189.

Friston KJ, Holmes AP, Worsley KJ, Poline J-B, Frith CD, Frackowiak RSJ. Statistical parametric maps in functional imaging: A general linear approach. Human Brain Mapping 1995;2:189–210.

Friston KJ, Josephs O, Zarahn E, Holmes AP, Rouquette S, Poline J. To smooth or not to smooth? Bias and efficiency in fMRI time-series analysis. Neuroimage 2000;12:196–208. [PubMed: 10913325]

Garavan H, Ross TJ, Murphy K, Roche RA, Stein EA. Dissociable executive functions in the dynamic control of behavior: Inhibition, error detection, and correction. Neuroimage 2002;17:1820–1829. [PubMed: 12498755]

Genovese CR, Lazar NA, Nichols T. Thresholding of statistical maps in functional neuroimaging using the false discovery rate. Neuroimage 2002;15:870–878. [PubMed: 11906227]

Hampshire A, Owen AM. Fractionating attentional control using event-related fMRI. Cerebral Cortex 2006;16:1679–1689. [PubMed: 16436686]

Ito S, Stuphorn V, Brown JW, Schall JD. Performance monitoring by the anterior cingulate cortex during saccade countermanding. Science 2003;302:120–122. [PubMed: 14526085]

Kerns JG, Cohen JD, MacDonald AW III, Cho RY, Stenger VA, Carter CS. Anterior cingulate conflict monitoring and adjustments in control. Science 2004;303:1023–1026. [PubMed: 14963333]

Knoch D, Gianotti LR, Pascual-Leone A, Treyer V, Regard M, Hohmann M, et al. Disruption of right prefrontal cortex by low-frequency repetitive transcranial magnetic stimulation induces risk-taking behavior. Journal of Neuroscience 2006;26:6469–6472. [PubMed: 16775134]

Levitt H. Transformed up–down methods in psychoacoustics. Journal of the Acoustical Society of America 1970;49:467–477. [PubMed: 5541744]

Li C-SR, Huang C, Constable T, Sinha R. Imaging response inhibition in a stop signal task—Neural correlates independent of signal monitoring and post-response processing. Journal of Neuroscience 2006;26:186–192. [PubMed: 16399686]

Li C-SR, Milivojevic V, Kemp K, Hong K, Sinha R. Performance monitoring and stop signal inhibition in abstinent patients with cocaine dependence. Drug and Alcohol Dependence 2006;85:205–212. [PubMed: 16725282]

Liotti M, Pliszka SR, Perez R, Kothmann D, Woldorff MG. Abnormal brain activity related to performance monitoring and error detection in children with ADHD. Cortex 2005;41:377–388. [PubMed: 15871602]

Liston C, Matalon S, Hare TA, Davidson MC, Casey BJ. Anterior cingulate and posterior parietal cortices are sensitive to dissociable forms of conflict in a task-switching paradigm. Neuron 2006;50:643–653. [PubMed: 16701213]

Logan GD, Cowan WB. On the ability to inhibit thought and action: A theory of an act of control. Psychological Review 1984;91:295–327.

MacDonald AW III, Cohen JD, Stenger VA, Carter CS. Dissociating the role of the dorsolateral prefrontal and anterior cingulate cortex in cognitive control. Science 2000;288:1835–1838. [PubMed: 10846167]

Mai, JK.; Paxinos, G.; Asheuer, JK. Atlas of the human brain. 2nd ed.. Academic Press; New York: 2003.

Penny, W.; Holmes, AP. Random-effects analysis.. In: Frackowiak, SJ.; Ashburner, JT.; Penny, WD.; Zeki, S.; Friston, KJ.; Price, CJ., et al., editors. Human brain function. Elsevier; San Diego: 2004. p. 843-850.

Rabbit PMA. Errors and error correction in choice–response tasks. Journal of Experimental Psychology 1966;71:264–272. [PubMed: 5948188]

Rahm B, Opwis K, Kaller CP, Spreer J, Schwarzwald R, Seifritz E, et al. Tracking the subprocesses of decision-based action in the human frontal lobes. Neuroimage 2006;30:656–667. [PubMed: 16256375]

Ridderinkhof KR, Ullsperger M, Crone EA, Nieuwenhuis S. The role of the medial frontal cortex in cognitive control. Science 2004;306:443–447. [PubMed: 15486290]

Schachar RJ, Chen S, Logan GD, Ornstein TJ, Crosbie J, Ickowicz A, et al. Evidence for an error monitoring deficit in attention deficit hyperactivity disorder. Journal of Abnormal Child Psychology 2004;32:285–293. [PubMed: 15228177]

Shafritz KM, Kartheiser P, Belger A. Dissociation of neural systems mediating shifts in behavioral response and cognitive set. Neuroimage 2005;25:600–606. [PubMed: 15784439]

Swainson R, Cunnington R, Jackson GM, Rorden C, Peters AM, Morris PG, et al. Cognitive control mechanisms revealed by ERP and fMRI: Evidence from repeated task-switching. Journal of Cognitive Neuroscience 2003;15:785–799. [PubMed: 14511532]

Ullsperger M, von Cramon DY. Neuroimaging of performance monitoring: Error detection and beyond. Cortex 2004;40:593–604. [PubMed: 15505969]

Van Veen V, Carter CS. The timing of action-monitoring processes in the anterior cingulate cortex. Journal of Cognitive Neuroscience 2002;14:593–602. [PubMed: 12126500]

Wager TD, Smith EE. Neuroimaging studies of working memory: A meta-analysis. Cognitive, Affective, and Behavioral Neuroscience 2003;3:255–274.

Wagner AD. Working memory contributions to human learning and remembering. Neuron 1999;22:19–22. [PubMed: 10027285]

Walton ME, Devlin JT, Rushworth MF. Interactions between decision making and performance monitoring within prefrontal cortex. Nature Neuroscience 2004;7:1259–1265.

Weissman DH, Roberts KC, Visscher KM, Woldorff MG. The neural bases of momentary lapses in attention. Nature Neuroscience 2006;9:971–978.

Yarkoni T, Gray JR, Chrastil ER, Barch DM, Green L, Braver TS. Sustained neural activity associated with cognitive control during temporally extended decision making. Brain Research, Cognitive Brain Research 2005;23:71–84. [PubMed: 15795135]

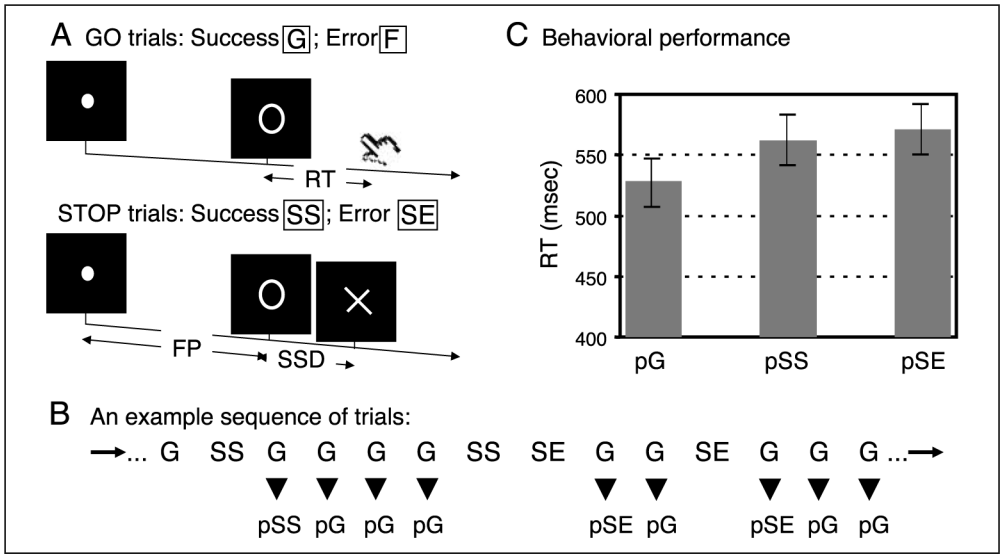

Figure 1.

(A) Stop signal paradigm. In "go" trials (75%), observers responded to the go signal (a circle), and in "stop" trials (25%), they had to withhold the response when they saw the stop signal (an X). In both trials, the go signal appeared after a randomized time interval between 1 to 5 sec (the fore-period or FP, uniform distribution) following the appearance of the fixation point. The stop signal followed the go signal by a time delay—the stop signal delay (SSD). The SSD was updated according to a staircase procedure, whereby it increased and decreased by 64 msec following a stop success and stop error trial, respectively. We distinguished go success (G: 97.1 ± 2.7%, mean ± *SD*) and go error (F: 2.9%), and stop success (SS: 50.3 ± 2.6%) and stop error (SE: 49.7%) trials during the task. (B) Go successes were further distinguished by their preceding trial; thus G trials preceded by a G, SS, and SE trial were indicated by pG, pSS, and pSE trials, respectively. Depending on whether they increased or did not increase in RT, compared to the mean RT of all preceding pG trials, pSS and pSE trials were further grouped into pSSi and pSSni, and pSEi and pSEni trials, respectively (not shown here; see Methods). (C) Both pSS and pSE trials showed prolonged RT, compared to pG trials, whereas pSS and pSE trials did not differ in RT. Data bars show median RT (mean ± S.E.) across all 40 subjects.

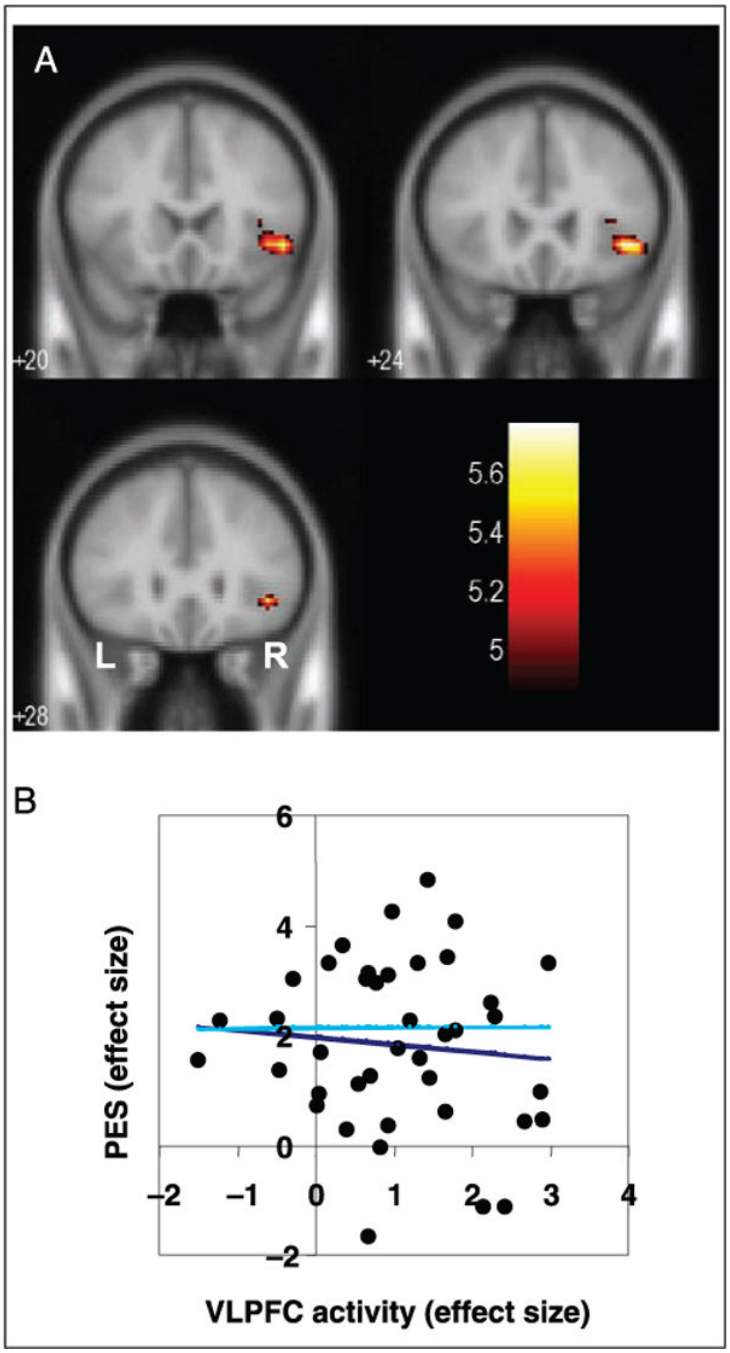

Figure 2.

(A) At a threshold of $p < .05$, corrected for multiple comparisons, the right ventrolateral prefrontal cortex (VLPFC) showed greater activation during post-error go trials with RT slowing (pSEi), compared to post-error go trials without RT slowing (pSEni). BOLD contrasts are superimposed on a T1 structural image in coronal sections from $y = 20$ to 28 mm. Adjacent sections are 4 mm apart. Color bar represents voxel t value. (B) The effect size of the post-error slowing (PES) in RT did not correlate with VLPFC activity in linear regression (dark blue: all 40 observers; light blue: all but 4 observers who showed a negative PES).

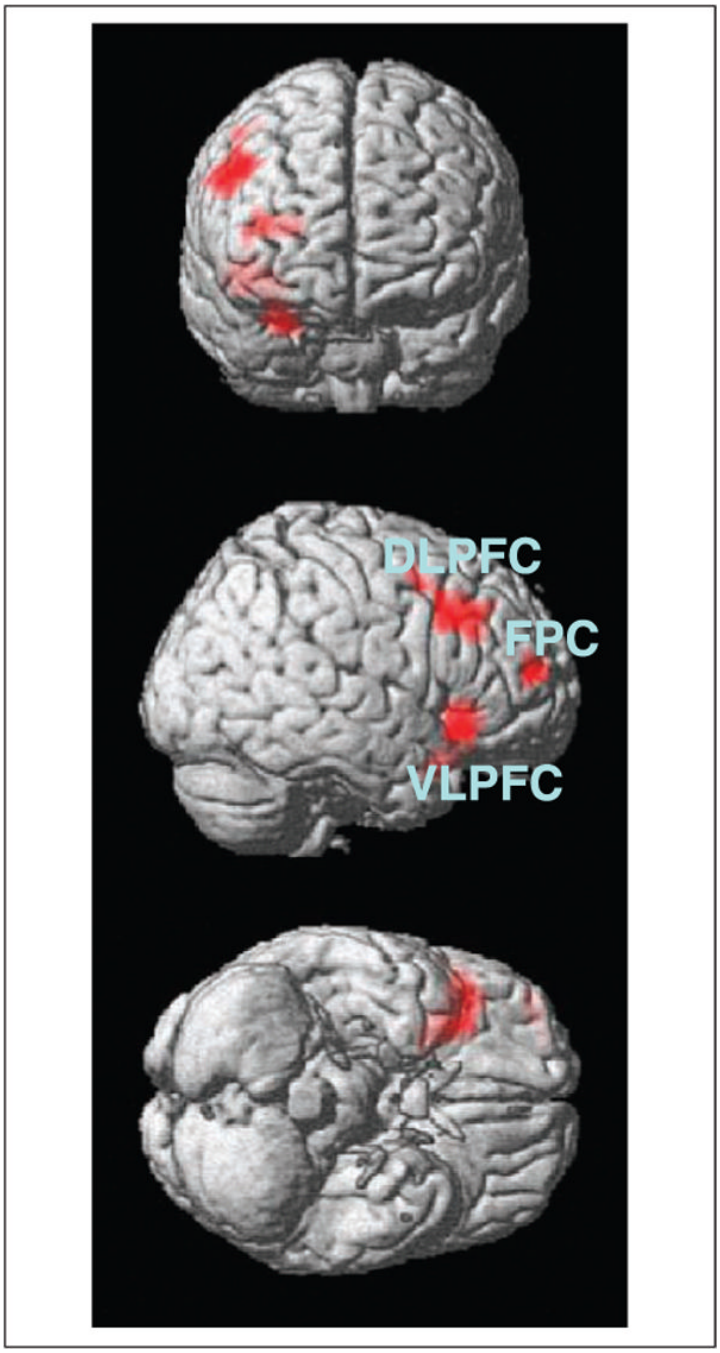

Figure 3.
Regions showing greater activation during pSE slowing compared to pSS slowing are rendered on a brain surface (front, side, and bottom of the brain, from top to bottom). These regions include, in the order of statistical significance, the right ventrolateral prefrontal cortex (VLPFC), the dorsolateral prefrontal cortex (DLPFC), and the fronto-polar cortex (FPC).

Table 1

a. General Performance in the Stop Signal Task

go RT (msec)	*%go*	*%stop*	*SSRT (msec)*	*Critical SSD (msec)*
547 ± 115	97.1 ± 2.7	50.3 ± 2.6	216 ± 32	332 ± 124

b. pSE and pSS Trials

	pSEi	*pSEni*	*pSSi*	*pSSni*
SSD of SE (SS) trials (msec)	355 ± 122	368 ± 142	311 ± 121	309 ± 123
RT of SE trials (msec)	490 ± 110	499 ± 126	NA	NA

%go and %stop = percentage of successful go and stop trials; SSRT = stop-signal reaction time; all numbers are mean ± standard deviation. pSEi (pSEni) = post-stop error trials with (without) RT slowing; pSSi (pSSni) = post-stop success trials with (without) RT slowing; SSD = stop signal delay; NA = not applicable.

Table 2

Regional Brain Activation of pSEi > pSEni

Cluster Size (Voxels)	*VoxelZ Value*	*MNI Coordinate (mm)*			*Side*	*Identified Region*
		x	*y*	*z*		
157	4.87	44	24	−4	R	Ventrolateral prefrontal G
	4.37	36	20	8	R	Ventrolateral prefrontal G
52	4.17	−32	20	12	L	Ventrolateral prefrontal G
	3.81	−44	16	−4	L	Ventrolateral prefrontal G
10	3.71	24	60	12	R	Frontopolar G
14	3.60	44	52	12	R	Middle frontal G

$p < .05$, corrected for FDR, and 5 voxels in extent; G = gyrus; 1 voxel = 64 mm^3.